Magnetically-Driven Activity in the Solar Corona: A Path to Understanding the Energetics of Astrophysical Plasmas

Sarah Gibson[1,2], Tim Bastian[3], Haosheng Lin[4], B. C. Low[2], Steve Tomczyk[2]

A report initiated by the AURA Solar Decadal Committee[5]

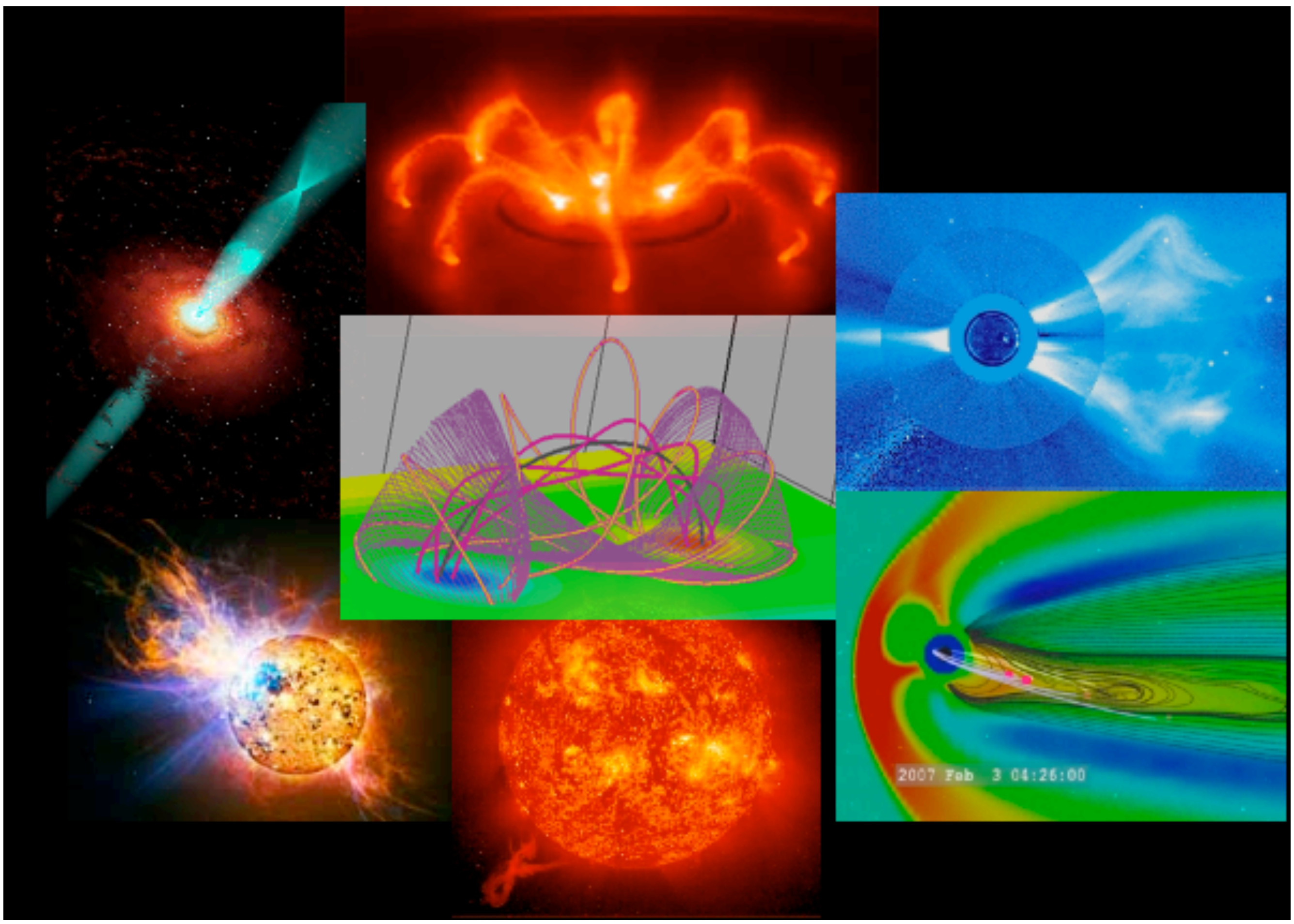

[1] sgibson@ucar.edu (corresponding author)
[2] NCAR/HAO, p.o. box 3000, Boulder, CO, 80301-3000
[3] National Radio Astronomy Observatory
[4] University of Hawaii
[5] http://www.aura-astronomy.org/nv/Solar%20Decadal%20Committee/Committee%20Membership%20and%20Mandate.pdf

Core question: *What will breakthrough observations of magnetic fields in the Sun's corona teach us about the storage and explosive release of magnetic energy in astrophysical plasmas?*

Background

Magnetism is important throughout the physical universe. Magnetohydrodynamic (MHD) and kinetic plasma processes have been studied in diverse astrophysical environments ranging from the Sun, through galactic molecular clouds, to black-hole accretion disks[1]. The storage and release of magnetic energy is a universal process of plasma astrophysics, likely to occur where there are driving forces and multiple scales[2]. Magnetic reconnection is thought to play a central role in energy conversion: energy stored in large-scale magnetic fields may be rapidly released as oppositely–directed magnetic fields are driven towards each other and topologically rearranged. The conditions under which magnetic reconnection is able to occur may be the deciding factor on how magnetic energy can be stored and ultimately released in a variety of plasma physical systems, including galaxies, stars, magnetospheres, and laboratory experiments[3]. One dramatic and well-studied example of reconnection-driven energy release is a solar flare. Flares on other stars have also been observed that are (presumably) analogous, but orders of magnitude stronger in luminosity and temperature[4]. In order to understand the mechanisms responsible for the implied large conversion of energy in stellar activity and related astrophysical processes, we must first understand magnetic energy storage and release at the Sun.

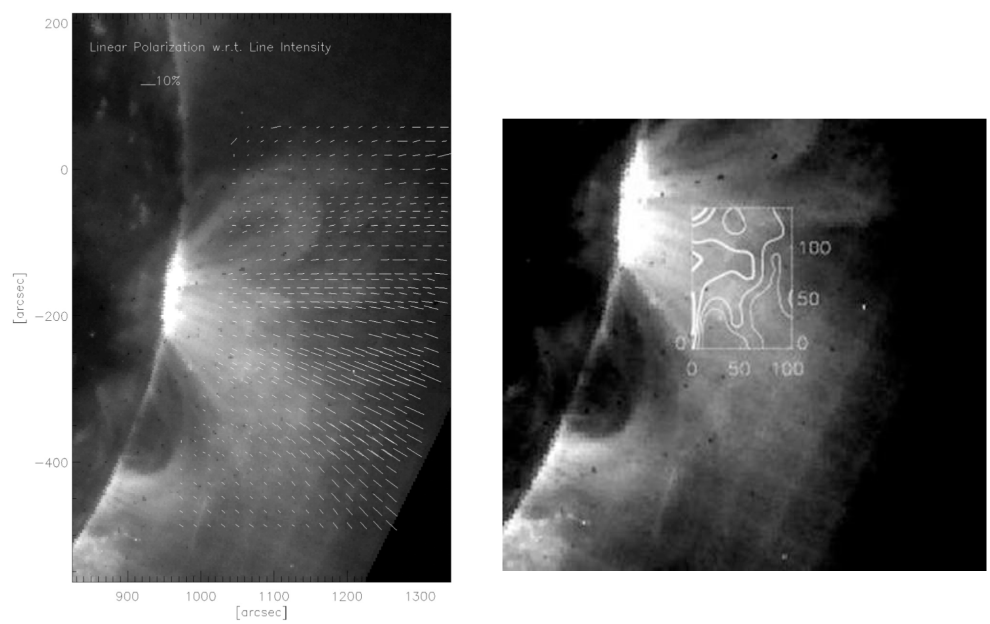

Figure 1. Measurement of coronal magnetic fields. Spatially resolved polarimetric measurements of an infrared forbidden iron line, as obtained by the Optical Fiber-bundle Imaging Spectropolarimeter (OFIS) on the 46-cm Solar Observatory for Limb Active Regions and Coronae (SOLARC) coronagraph at Haleakala. At left is the direction of the magnetic field in the plane of the sky, derived from linear polarization measurements and superposed on an SOHO/EIT EUV image for context (only a portion of the southwest quadrant of the solar disk is shown). At right is a contour plot of the line-of-sight magnetic field strength determined from circular polarization. The contours are 5G, 3G, and 1G.

Figure 2. Snapshot image of synchrotron emission from MeV electrons entrained in the magnetic field of expanding coronal mass ejection (CME) loops. The event of 1998 April 20 was observed by the Nançay Radioheliograph at 5 frequencies between 150-450 MHz. Fits to the multi-frequency imaging data for this CME were used to infer magnetic field strength and ambient density at locations in the CME loops indicated by the white dots. The magnetic field was found to vary from approximately 0.3 to 1.5 G.

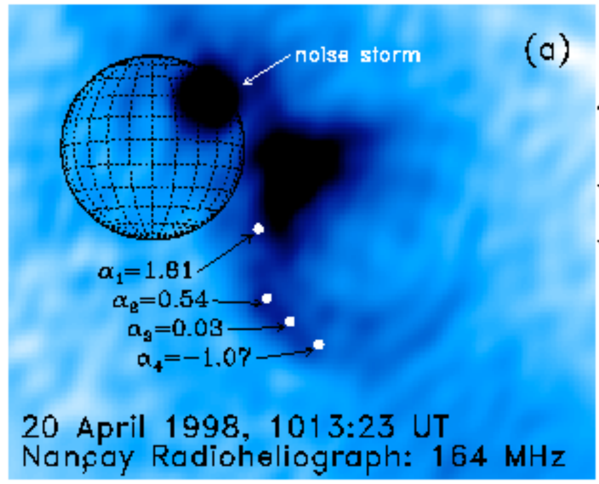

The Sun is a laboratory for probing such astrophysical processes: its proximity allows us to observe solar magnetism in spatial detail not possible elsewhere in astrophysics, and at the characteristic time scales of magnetically-driven phenomena. For decades now we have observed the vector magnetic field at the solar surface (photosphere) with ever-increasing spatial and temporal resolution[5]. From these observations we have learned and continue to learn about how magnetic flux emerges and evolves over multiple time scales. Magnetic fields in the solar atmosphere, especially in the corona, dominate force balance, controlling the structure and dynamics of coronal plasma. Until very recently, our knowledge of these coronal magnetic fields was limited to what we could infer from observations at the solar surface and coronal plasma observations. We are currently at a watershed moment: Infrared and radio observations have begun obtaining measurements of the coronal magnetic field **(Figures 1-2)**[6]**.** Such observations are bound to be paradigm-changing, since we have reached a point where theories of solar coronal MHD have extended beyond what, up until now, has been possible to observationally test. **In this white paper we will describe how the new field of coronal magnetometry will lead to breakthroughs in our understanding of how magnetic energy is stored and released in solar eruptions.** Note that science white papers have also been submitted by **Bastian *et al.*** and **White *et al.*,** which discuss how the new coronal magnetometry will likewise advance our knowledge of particle acceleration and stellar activity, respectively.

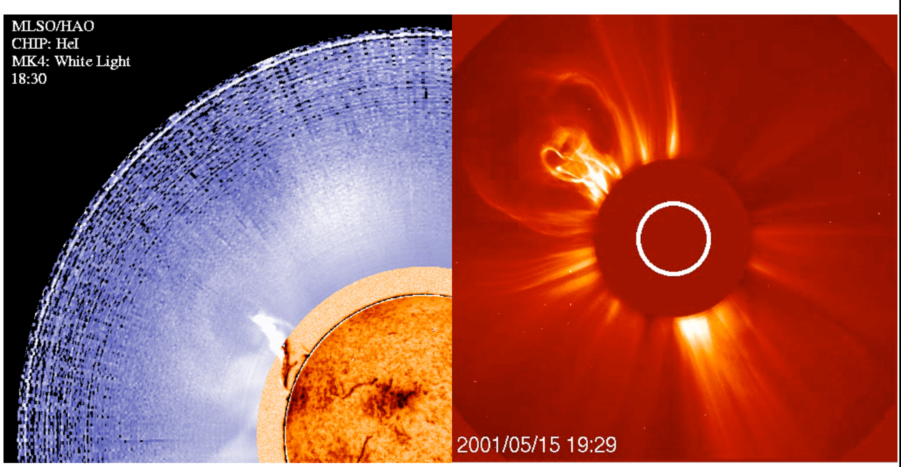

Figure 3: Coronal mass ejection (CME) on May 15, 2001, as observed by (left) Mauna Loa Solar Observatory (MLSO) and (right) SOHO LASCO. MLSO observations show that the core of the CME is an erupting prominence (inner, orange image): relatively cool, dense entrained in an expanding coronal magnetic field. Prominences are believed to store magnetic energy, existing stably for days or weeks before erupting.

Storage and release of magnetic energy in the corona

Coronal mass ejections (CMEs) and solar flares are episodic releases of thermal, radiative, and kinetic energies in the corona **(Figure 3)**. The energies released in each episode are gradually built up and stored in coronal magnetic fields via a process of magnetic flux transport from beneath the solar surface. We now identify questions of broad astrophysical relevance that could be uniquely addressed by the new observations of coronal magnetic fields.

What is the nature of pre-eruption, stable coronal hydromagnetic equilibria (stored magnetic energy)? Are there physically-defined thresholds of magnetic helicity/energy for the explosive transition between these equilibria? Observations of magnetic flux emergence through the photosphere, and of the resulting evolution of coronal plasma, indicate that magnetic energy is transferred in the form of sheared or twisted magnetic fields and stored in the coronal atmosphere[7]. Moreover, regions that are considered to contain significant coronal currents are common sites of eventual eruption (e.g., the prominence erupting in **Figure 3**). One set of theoretical models argues that a loss of equilibrium drives eruptions when a threshold for magnetic energy or helicity is passed: magnetic fields are twisted to the breaking-point[8]. Attempts have been made to quantify coronal magnetic energy and helicity by extrapolating photospheric fields, or by observing the time variation of vector photospheric fields[9]. However, such analyses make assumptions about how magnetic flux emerges through the photosphere and/or the distribution of coronal currents. The photosophere and corona are fundamentally different regimes: observations within the corona itself are required for a definitive calculation of magnetic energy and helicity at any given time.

Can we identify observationally and theoretically the specific and commonly occurring triggers for eruptions? Another class of model argues that eruptions occur in the presence of a particular magnetic topology, which is prone to explosive reconnection when driven by shearing motions and/or flux emergence at the photosphere[10]. Observations of coronal plasma and photospheric fields have been shown to be consistent with this picture[11], but without observations of coronal magnetic fields, it is not possible to distinguish between a topology-dependent model and one in which the eruption occurs because the magnetic energy/helicity has been pushed past a threshold. At present the primary means of probing coronal magnetic topology is via extrapolations from photospheric magnetic fields, which rely on many assumptions[12]. Direct coronal observations of magnetic topological features such as magnetic null points and current sheets are needed to clearly distinguish between models.

What MHD constraints determine the fraction of stored magnetic energy released in an eruption and the interplay between ideal and dissipative plasma processes in that energy release? Observations of repeated eruptions from a single solar active region indicate that free magnetic energy, i.e. the energy above a potential field, may be retained after each eruption. Numerical simulations have shown that when equilibrium is lost upon crossing the magnetic twist threshold for the kink instability, a new equilibrium can be found that still possesses substantial free magnetic energy[13]. Indeed, the magnetic energy that is released may not result in any significant loss of coronal mass or magnetic helicity. The released magnetic energy is partitioned into dissipation (e.g. flare heating), ideal bulk/kinetic motions of the CME and work done against solar gravity, and ordered, accelerated particle beams that may subsequently heat the atmosphere (see **Bastian *et al.*** white paper). Direct observations of coronal magnetic fields are needed to quantify the slow buildup of magnetic energy prior to eruption(s) and to establish what fraction of magnetic energy is released during eruption. Observations of CME dynamics, flare thermal emissions, and non-thermal processes can then be combined with topological information about the coronal field to deduce how magnetic energy has been transferred.

Coronal magnetometry

In order to answer these questions we need observations that pinpoint the strength and topology of the time-evolving vector coronal magnetic field. This is the domain of the emerging field of coronal magnetometry.

Magnetic field strength: We have described the importance of measuring magnetic energy in the corona: for this we need to know the magnitude of the magnetic field vector. For regions characterized by strong magnetic fields (> 150 G), radio thermal gyroresonance emission provides a means of measuring field strength as a function of position and time (**Figure 4**)[14]. At the solar limb, this optically-thick emission provides an unambiguous measure of field strength vs. height. On the solar disk, establishing the heights of gyroresonant surfaces requires a model for temperature. During solar eruptions, nonthermal gyrosynchrotron emission can also be fit to models to predict magnetic field strengths (see **Figure 2** and **Bastian *et al.*** white paper). Finally, for weaker fields, the magnitude of the magnetic field vector can be determined at the solar limb if both the longitudinal (line-of-sight) and transverse (plane-of-the sky) magnetic field strengths are independently determined, as we now describe.

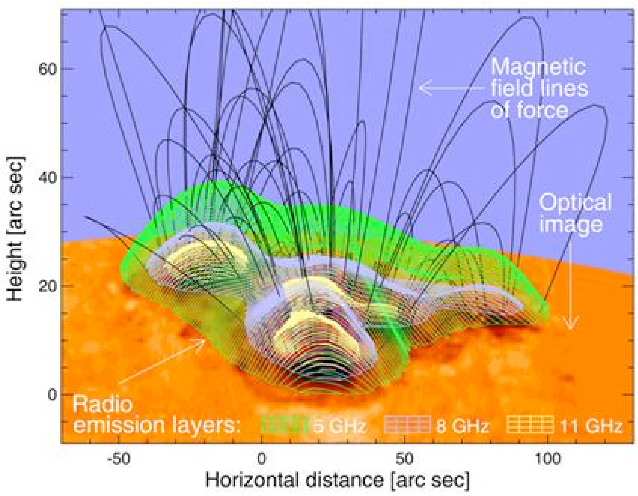

Figure 4. A perspective view of AR6615 (7 May 1991) is shown in white light continuum with extrapolated field lines. The three surfaces are the gyroresonant surfaces in the corona that will dominate the radio opacity at each of three radio frequencies: 5 GHz (B = 600 G), 8 GHz (B = 950 G) and 11 GHz (B = 1300 G), assuming σ=3.

Magnetic field direction: In order to quantify magnetic helicity, and to probe for topological features such as magnetic null points and current sheets, it is necessary to have information about the direction of the magnetic field vector. Observations in the infrared emission of magnetic dipole lines, like the FeXIII 1074.7 nm line, yield longitudinal (line-of-sight) magnetic field strength and plane-of-sky field orientation at the solar limb, integrated along the line of sight in the optically thin corona (as shown in **Figure 1**). We must note that the linear polarization of the infrared forbidden lines is insensitive to the field strength, therefore the full vector magnetic field cannot be measured directly. However, magneto-acoustic waves (as observed at both radio and infrared frequencies) may provide an independent diagnostic of transverse magnetic field strength when combined with density observations[15]. Alternatively, infrared measurements using the Zeeman effect and scattering polarization can yield full vector field information when the polarized light originates from a confined and localizable volume. In those cases, constraints can be placed on the inclination of the magnetic field and therefore the total field strength and direction[16]. Radio free-free emission presents another opportunity to probe longitudinal magnetic field, which it depends upon in combination with density-squared (integrated along the line of sight). The independent radio and infrared diagnostics of longitudinal fields are complementary: the infrared observations can probe magnetic fields to higher heights in the coronal atmosphere than the radio, while the radio observations, which do not require an occulting disk, provide information about the longitudinal field in the lower corona and chromosphere.

Other indicators of magnetic topology: The plane-of-sky field direction shown in **Figure 1** is determined from the linear polarization signal of scattered infrared radiation, subject to a 90 degree ambiguity. This ambiguity is due to the "Van Vleck" effect, which causes nulls of linear polarization to occur at a specific angle between the magnetic field and the solar vertical. On either side of the null, the polarization direction changes by 90˚. Identification of linear polarization nulls can be used for example to probe for the presence of current sheets[17]. Radio observations can provide a similar constraint: when radiation traverses a magnetic field wherein the longitudinal field component changes sign, the polarization of the radiation may reverse, depending on whether the coupling between the ordinary and extraordinary modes is strong or weak[18]. If observations are obtained simultaneously at multiple radio frequencies, a "depolarization sheet'" can be deduced above active regions, providing a three-dimensional constraint on the magnetic field: i.e., the locations where it is perpendicular to the line of sight.

***Tools and techniques*:** Many of the coronal field diagnostics we have described require information about density and/or temperature, and those that depend upon optically-thin emission are subject to superposition of structures along the observer's line of sight. For these reasons it is clear that it is important to make use of **forward modeling**, that is, the input of physical MHD quantities (e.g., vector magnetic field, density, temperature, and velocity) predicted by a model into a forward code designed to reproduce IR and radio coronal magnetographic observations. Such forward analyses could be used either to directly compare a model's prediction to observations, or more generally to test whether the observations can distinguish between different models[17.19]. Complementary **coronal plasma diagnostics**, as are obtained from white light coronagraph and EUV emission, are also important constraints. Finally, **stereoscopic inversions** may be employed to disentangle line-of-sight effects, providing the structures being so probed evolve on time scales longer than that of solar rotation.

Future projects

Observations using existing telescopes[6] (e.g. **Figures 1-2**) serve as proof of concept for coronal magnetometry, and will continue to be employed in developing tools and techniques. However, future progress requires further expansion of coronal magnetographic assets.

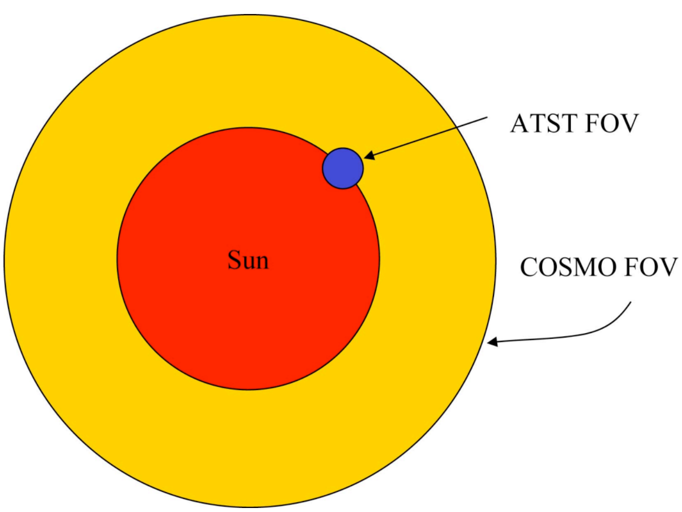

Two complementary telescopes will be used to obtain infrared coronal magnetic field diagnostics above the solar limb as described above. The ***Advanced Technology Solar Telescope (ATST)***[20] will do so with extremely high sensitivity, due to its four-meter aperture and subsequent low scattering. Calculations based on realistic background estimates show the ATST will reach a one-sigma error of 32 Gauss for the coronal magnetic field in a typical active region corona in a one-arcsecond pixel with only one second of integration. The ATST will thus be an excellent telescope for probing the coronal magnetic field of specific structures, such as active regions, prominences and their cavities, and coronal streamers, with extreme sensitivity and spatial/temporal resolution. The ***Coronal Solar Magnetism Observatory (COSMO)***[21] would obtain the same infrared coronal field diagnostics as ATST with lower sensitivity/resolution, but synoptically and covering the full corona above the limb. It would provide daily observations of the coronal magnetic field down to 1 Gauss over a 1° field of view and be operated 365 days per year, weather permitting, with a spatial resolution of 5” at a temporal cadence of 10-30 minutes. The full-sun COSMO observations would provide global context for the high-resolution but small field-of-view ATST observations. COSMO’s large field of view and synoptic nature would allow it to capture (i.e. not miss) many more eruptive events, and to provide observations both before and after eruptions.

The ***Frequency Agile Solar Radiotelescope (FASR)***[22] would sample the radio spectrum from 50 MHz (a wavelength of 6 m) to 21 GHz (a wavelength of just under 1.5 cm), probing plasma in the mid-chromosphere up to coronal heights (1.5-4 solar radii) both on the solar disk and above the solar limb. The coronal magnetic field would be measured or otherwise constrained using the radio coronal field diagnostics described above, all of which depend on broadband imaging spectroscopy, with spatial resolution of $20/\nu_{GHz}$ arcseconds (where ν_{GHz} is the frequency in GHz). As in the case of COSMO, FASR would provide synoptic/full-sun observations, greatly increasing the likelihood of obtaining observations before, during, and after eruptions. It would observe both on the disk and above the limb, with a temporal cadence of less than a second.

Conclusions

The coronal magnetic field data that will be obtained over the next decade will be unprecedented, and new discoveries are sure to be made. There are challenges to be met in interpreting these data, but a concerted effort has already begun to develop tools and techniques for addressing these challenges in a manner that spans wavelength regimes and brings together complementary radio and infrared diagnostics. In combination with coronal plasma observations and modeling, this new coronal magnetometry has the potential to bust coronal physics as it now exists wide open, by shedding light on long-standing mysteries of how coronal magnetic fields drive solar activity. The insight we will gain into how magnetic energy is stored and ultimately released in spectacular solar eruptions is key to understanding a wide range of analogous dynamic phenomena throughout astrophysics.

References

1) **Turbulence and Magnetic Fields in Astrophysics**, 2003, edited by E. Falgarone, and T. Passot, Springer Berlin/Heidelberg, *Lecture Notes in Physics*, vol. 614; **Modeling the galactic center nonthermal filament as magnetized wakes**, 2002, R. B. Dahlburg, G. Einaudi, T. N. LaRosa, and S. N. Shore, *ApJ*, 568, 220-225; **A variable efficiency for thin-disk black hole accretion**, 2001, C. S. Reynolds, P. J. Armitage, *ApJ*, 561, L81-L84; **Magnetic floods: A scenario for the variability of the microquasar GRS 1915+105,** 2004, M. Tagger, P. Varnière, J. Rodriguez, R. Pellat, *ApJ*, **607,** 410-419
2) **Plasma physics of the local cosmos**, 2004, Committee on Solar and Space Physics, National Academies Press, Washington D. C., p. 57-64
3) **Production of the large scale superluminal ejections of the microquasar GRS 1915+105 by violent magnetic reconnection**, 2005, De Gouveia Dal Pino, E. M., and Lazarian, A., *A&A*, 441, 845-753; **Energy extraction from a rotating black hole by magnetic reconnection in the ergosphere**, 2008, Koide, S. and Arai, K., *ApJ*, 682, 1124-1133; **X-ray flares in Orion young stars. I. Flare characteristics**, 2008, Getman, K. V., Feigelson, E. D., Broos, P. S., Micela, G. and Garmire, G. P., *ApJ*, 688. 418-436; **Magnetospheric accretion and winds on the T Tauri star SU Aurigae. Multi-spectral line variability and cross-correlation analysis,** 2000, Oliveira, J. M., Foing, B. H., van Loon, J. Th., Unruh, Y. C., *A&A*, 362, 615-627; **Recent in-situ**

observations of magnetic reconnection near-Earth space, 2008, Paschmann, G., *GRL*, 35, L19109, doi:10.1029/2008GL035297; **New insights into dissipation in the electron layer during magnetic reconnection**, 2008, Ji, H., Ren, Y., Yamada, M., Dorfman, S., Daughton, W., and Gerhardt, S. P., *GRL*, 35, L13106, doi:10.1029/2008GL034538

4) **X-ray astronomy of stellar coronae,** 2004, Guedel, M., *A&AR*, 12, 71; **Scaling laws of solar and stellar flares,** 2008, Aschwanden, M. J., Stenr, R. A., Guedel, M., *ApJ*, 672, 659
5) **The Solar Optical Telescope for the *Hinode* mission: an overview** [and references therein]**,** 2008, Tsuneta, S. and 24 co-authors *Solar Phys.,* 249, 167-196
6) **The coronal mass ejection of 1998 April 20: Direct imaging at radio wavelengths**, 2001, Bastian, T. S., Pick, M., Kerdraon, A., Maia, D., and Vourlidas, A., *ApJ*, 558, L65-L69; **Coronal magnetic field measurements**, 2004, Lin, H., Kuhn, J. R., and Coulter, R., *ApJ*, 613, L177-L180; **An instrument to measure coronal emission line polarization**, 2008, Tomczyk, S., *et al., Solar Phys*., 247, 411
7) **Evidence for current-carrying emerging flux**, 1996, Leka, K. D., Canfield, R. C., McClymont, A. N., van Driel-Gesztelyi, L., *ApJ,* 462, 547-560; **Sigmoidal morphology and eruptive solar activity**, 1999, Canfield, R. C., Hudson, H. S., and McKenzie, D. E., *GRL*, 26, 627-630
8) **A catastrophe mechanism for coronal mass ejections,** 1991, Forbes, T. G. and Isenberg, P. A., *ApJ,* 373, 294-307; **A twisted flux rope model for coronal mass ejections and two-ribbon flares**, 2000, Amari, T., Luciani, J. F., Mikic, Z., and Linker, J., *ApJ*, 529, L49; **Magnetic field confinement in the corona: the role of magnetic helicity accumulation**, 2006, Zhang, M. Flyer, N., and Low, B. C., *ApJ*, 644, 575-586; **Onset of coronal mass ejections due to loss of confinement of coronal flux ropes**, 2007, Fan, Y., and Gibson, S. E., *ApJ*, 668, 1232-1245
9) **Magnetic energy and helicity budgets in the active region solar corona. I. Linear force-free approximation** [and references therein], 2007, Georgoulis, M. K. and LaBonte, B. J., *ApJ,* 671, 1034-1050
10) **A model for solar coronal mass ejections**, 1999, Antiochos, S. K., DeVore, C. R., Klimchuk, J. A., *ApJ*, 510, 485-493
11) **The topology and evolution of the Bastille Day flare**, 2000, Aulanier, G., DeLuca, E. E., Antiochos, S. K., McMullen, R. A., Golub, L., *ApJ*, 540, 1126-1142
12) **Nonlinear force-free modeling of coronal magnetic fields. II. Modeling a filament arcade and simulated chromospheric and photospheric vector fields**, 2008, Metcalf, T. R. and 8 co-authors, *Solar Phys*., 247, 269-299
13) **Confined and ejective eruptions of kink-unstable flux ropes,** 2005, Toeroek, T., Kliem, B., *ApJL*, 630, L97-L100; **The partial expulsion of a magnetic flux rope**, 2006, Gibson, S. E., Fan, Y., ApJL, 636, L65-68
14) Image courtesy J. Lee/NJIT; Force-free extrapolation of photospheric fields by Z. Mikic
15) **Alfven waves in the solar corona**, 2007, Tomczyk, S., McIntosh, S. W., Keil, S. L., Judge, P. G., Schad, T., Seeley, D. H., and Edmondson, J., *Science*, 317, 5842, 1192-1196
16) **Spectral lines for polarization measurements of the coronal magnetic field. V. Information content of magnetic dipole lines**, 2007, Judge, P. G., *ApJ*, 662, 677-690
17) **Spectral lines for polarization measurements of the coronal magnetic field. IV. Stokes signals in current-carrying fields**, 2006, Judge, P. G., Low, B. C., and Casini, R., *ApJ*, 651, 1229-1237
18) **Coronal magnetography of solar active region 8365 with the SSRT and NoRH radio heliographs**, 2005, Riyabov, B. I., Maksimov, V. P., Lesovoi, S. V., Shibasaki, K., Nindos, A. Pevstov, A., *Solar Phys.,* 226, 223-237
19) **Observational test of coronal magnetic field models. I. Comparison with potential field model**, 2008, Lin, Y., Lin, H., *ApJ,* 680, 1496
20) http://atst.nso.edu/
21) http://www.cosmo.ucar.edu/
22) http://www.fasr.org/